# Simulations and Reconstructions of Aircraft Flights and Accidents

**Grzegorz Kowaleczko**
Military University of Technology
ul. Kaliskiego 2, 00-908 Warsaw, Poland
tel. +48 22 6839046

e-mail: kowaleczko@wmt.wat.edu.pl

## *ABSTRACT*

*The paper presents exemplary results of numerical simulations focused on numerical simulations and reconstructions of aircraft flights and accidents. These works were carried out for both fixed-wing and rotary-wing aircraft during last seven years at the Institute of Aviation Technology. These investigations were mainly theoretical but some of them were verified on the basis of data recorded during flight tests.*

*All investigations were founded on the classic model of an aircraft, which was treated as a rigid body [1].*

*Spatial manoeuvres of aircraft were modelled by making use of inverse simulations /[1], [2], [3]/. This method allows to determine control necessary to perform an assumed manoeuvre.*

*Some main results are presented for both normal flight and aircraft crash.*

### Notations

**For an aeroplane:**

$\overline{X} = (V, \alpha, \beta, P, Q, R, \Theta, \Phi, \Psi, x_g, y_g, z_g)$ - vector of flight parameters

$V$ - velocity of flight

$\alpha, \beta$ - angle of attack, sideslip angle, respectively

$P, Q, P$ - angular velocity components (body axes)

$\Theta, \Phi, \Psi$ - Euler angles of fuselage

$x_g, y_g, z_g$ - position coordinates

$\overline{S} = (T_c, \delta_H, \delta_L, \delta_V)$ - vector of control parameters

$T_c$ - thrust of engines

$\delta_H, \delta_L, \delta_V$ - deflections of elevator, aileron and rudder, respectively

**For a helicopter:**

$\overline{X} = (U, V, W, P, Q, R, \Theta, \Phi, \Psi, x_g, y_g, z_g, \omega)$ - vector of flight parameters

$U, V, W$ - linear velocity components (body axes),

Kowaleczko, G. (2005) Simulations and Reconstructions of Aircraft Flights and Accidents. In *Flight Test – Sharing Knowledge and Experience* (pp. 22-1 – 22-22). Meeting Proceedings RTO-MP-SCI-162, Paper 22. Neuilly-sur-Seine, France: RTO. Available from: http://www.rto.nato.int/abstracts.asp.

$\omega$ - angular velocity of the main rotor

$\bar{S} = (\theta_0, \kappa_s, \eta_s, \phi_{tr})$ - vector of control parameters

$\theta_0$ - collective pitch of a main rotor

$\kappa_s$ $\eta_s$ - longitudinal and lateral cyclic pitch angles

$\phi_{tr}$ - collective pitch of a tail rotor

## 1.0 MATHEMATICAL MODEL OF OBJECTS

Manoeuvres of a helicopter and an aeroplane were considered. Both objects were treated as rigid bodies with six degrees of freedom. In both cases dynamics was described by sets of nonlinear differential equations. They can be written symbolically in the form:

$$\mathbf{A}(t,X)\frac{d\bar{X}}{dt} + \bar{B}(t,X) = \bar{F}(t,X,\bar{S}) \qquad (1.1)$$

Vector $X \in \Re^{n_x}$ is the vector of flight parameters and $\bar{S} \in \Re^{n_s}$ is the vector of control parameters.

Additionally, for a helicopter, dynamics of a blade flapping motion is taken into account. In this case the set (1.1) should be complemented by the following set of nonlinear algebraic equations:

$$\hat{L}(\bar{X},\bar{S},\bar{\beta})\bar{\beta} = \bar{F}(\bar{X},\bar{S},\bar{\beta}) \qquad (1.2)$$

where $\bar{\beta} = (a_0, a_1, b_1)$ is a vector determining orientation of the cone of the main rotor in relation to the fuselage.

## 2.0 INVERSE SIMULATION ALGORITHM

The set (1.1) is transformed to the following form:

$$\frac{d\bar{X}}{dt} = \dot{\bar{X}} = \bar{G}(t,X,\bar{S}) \qquad (1.3)$$

which could be integrated using one of the numerical methods (for instance the Runge-Kutta method).

Vector $\bar{G}$ is equal to:

$$\bar{G} = \mathbf{A}^{-1}(\bar{F} - \bar{B}) \qquad (1.4)$$

The output vector $\bar{Y} \in \Re^{n_y}$ is uniquely determined by the vector of flight parameters $\bar{X}$:

$$\bar{Y} = \bar{D}(\bar{X}) \qquad (1.5)$$

In the present considerations both vectors are the same:

$$\bar{Y} = \bar{X} \qquad (1.6)$$

The set (1.3) is completed by the following initial conditions:

$$\bar{X}(t_0) = \bar{X}_0 \qquad (1.7)$$

As it was mentioned, in the considered case, the fundamental problem is to determine the control vector $\bar{S}(t)$ for the defined output vector $\bar{Y}_z(t)$, which describes constraints of the object motion.

Problem is made discrete for successive time points $t_0, \ldots t_k, t_{k+1}, \ldots t_N$. For each instant $t_{k+1}$, the vector $\bar{Y}_z(t_{k+1})$ is defined by constraints of motion. The vector $\bar{X}(t_{k+1})$ is also calculated as a result of integration of the set (1.3) in the time interval from $t_k$ to $t_{k+1}$. This interval is determined in the way which preserves the stability of final solution. Because the described procedure requires the one constant time step and because of a nonlinearity of the problem, this step is determined by numerical experiments. This means that several simulations should be performed with decreasing time intervals up to the moment when two convergent solutions are obtained. The method is in compliance with the Runge-Kutta method with different time interval. The time interval is dependent upon every individual problem. According to (1.3), because the derivative $\frac{d\bar{X}}{dt}$ depends on the control vector $\bar{S}(t_k)$, the calculated value $\bar{X}(t_{k+1})$ also depends on this control vector. The vector $\bar{Y}(t_{k+1})$ determined on the basis of relation (1.5) has to be equal to specified value $\bar{Y}_z(t_{k+1})$. Difference between the calculated value of the vector $\bar{Y}(t_{k+1})$ and the constrained vector $\bar{Y}_z(t_{k+1})$ is the basis for the calculation of a corrected value of control the vector $\bar{S}(t_k)$.

This procedure has an iterative character. It means that for each time point $t_k$, a finite number of iterations is performed till the assumed compatibility between vectors $\bar{Y}$ and $\bar{Y}_z$ is obtained. In the *i*-th iteration, the following operations are performed:

1. On the basis of a known $\bar{X}(t_k)$ and $\bar{S}^{(m)}(t_k)$ making use of (1.3) the derivative is calculated:

$$\dot{\bar{X}}^{(m)}(t_k) = \bar{G}[t_k, \bar{X}(t_k), \bar{S}^{(m)}(t_k)] \qquad (1.8)$$

2. The value of flight parameters and output vector at the time point $t_{k+1}$ is determined by numerical integration of relation (1.8):

$$\bar{X}^{(m)}(t_{k+1}) = \bar{X}(t_k) + \int_{t_k}^{t_{k+1}} \dot{\bar{X}}^{(m)}(t_k)dt \qquad (1.9)$$

$$\bar{Y}^{(m)}(t_{k+1}) = \bar{D}[\bar{X}^{(m)}(t_{k+1})] \qquad (1.10)$$

3. The difference between defined output vector $\bar{Y}_z(t_{k+1})$ and the vector calculated from (1.10) is determined:

$$\Delta\bar{Y}^{(m)}(t_{k+1}) = \bar{Y}_z(t_{k+1}) - \bar{Y}^{(m)}(t_{k+1}) \qquad (1.11)$$

If this difference is smaller than defined accuracy $\varepsilon_{\bar{Y}}$, calculations are continued at next time point $t_{k+2}$. The vector of flight parameters and the control vector determined at time $t_{k+1}$ are taken as an initial data. If this difference $\Delta\bar{Y}^{(m)}(t_{k+1})$ is greater then $\varepsilon_{\bar{Y}}$ the improved value of control vector $\bar{S}^{(m+1)}(t_k)$ is calculated. For this purpose the Newton method is applied. According to this method an expression for $\bar{S}^{(m+1)}(t_k)$ is as follows:

$$\bar{S}^{(m+1)}(t_k) = \bar{S}^{(m)}(t_k) + \mathbf{J}^{-1}\Delta\bar{Y}^{(m)}(t_{k+1}) \quad (1.12)$$

where $\mathbf{J}$ is the Jakobian. Its elements are determined by the formula:

$$J_{ij}(t_k) = \frac{\partial[\Delta Y_i^{(m)}(t_{k+1})]}{\partial S_j^{(m)}(t_k)} = \frac{\partial Y_i^{(m)}(t_{k+1})}{\partial S_j^{(m)}(t_k)} \quad (1.13)$$

Because the considered problem is solved numerically, then the following differential scheme is applied:

$$J_{ij}(t_k) = \frac{Y_i^{(m)}[t_{k+1}, S_j^{(m)}(t_k) + \delta S_j^{(m)}] - Y_i^{(m)}[t_{k+1}, S_j^{(m)}(t_k) - \delta S_j^{(m)}]}{2\delta S_j^{(m)}} \quad (1.14)$$

The expression (1.12) is a result of the following procedure:

The output vector $\bar{Y}^{(m)}(t_{k+1})$ is calculated at the time point $t_{k+1}$ at *m*-th iteration. It depends on the flight parameters vector $X(t_k)$ and the control vector $\bar{S}^{(m)}(t_k)$, which are determined at the previous time point $t_k$.

If the calculations are performed again for a modified value of the control vector:

$$\bar{S}^{(m+1)}(t_k) = \bar{S}^{(m)}(t_k) + \Delta\bar{S}^{(m)}(t_k) \quad (1.15)$$

a new value of the output vector $\bar{Y}^{(m+1)}(t_{k+1})$ for the *(m+1)*-th iteration is obtained. Making use of the Taylor series and taking into account only linear part of the expansion in series, it can be assumed that:

$$\bar{Y}^{(m+1)}(t_{k+1}) = \bar{Y}^{(m)}(t_{k+1}) + \mathbf{J}\Delta\bar{S}^{(m)}(t_k) \quad (1.16)$$

where Jacobian elements are determined by relations (1.13) and (1.14). Using relation (1.16), after elementary transformations, one can obtain formula (1.12), which allows to calculate the control vector at time $t_k$ for the *(m+1)*-th iteration $\bar{S}^{(m+1)}(t_k)$. It is assumed that the calculated value of the output vector $\bar{Y}^{(m+1)}(t_{k+1})$ has to be equal to the determined value $\bar{Y}^{(m+1)}(t_{k+1}) = \bar{Y}_z(t_{k+1})$. It is also taken into account in relation (1.11).

## 3.0 VERIFICATION OF THE METHOD

To verify the mathematical model of analysed objects and the inverse technique, used in simulations, results of them were compared with data recorded in flight trials. It was done for aeroplanes [4] and the helicopter [5], [6]. Figures 1÷8 present exemplary results of comparison (1 – recorded data, 2 – computed data). In this case an airplane reaction to the impulse deflection of the elevator was tested.

The flight velocity and all three angular velocities were used as constrains. Because they were recorded not very precisely their time courses were modified – „the zero level" was changed. Fig.1 shows recorded and simulated flight velocity, Fig.2 – rolling velocity, Fig.3 – pitching velocity, Fig.4 – yawing velocity.

Figures 5÷8 confirm, that the used inverse method and mathematical model of the airplane are correct – recorded and computed: angle of attack (Fig.5), altitude of flight (Fig.6), overload factor (Fig.7) and elevator angle (Fig.8) are in satisfactory agreement.

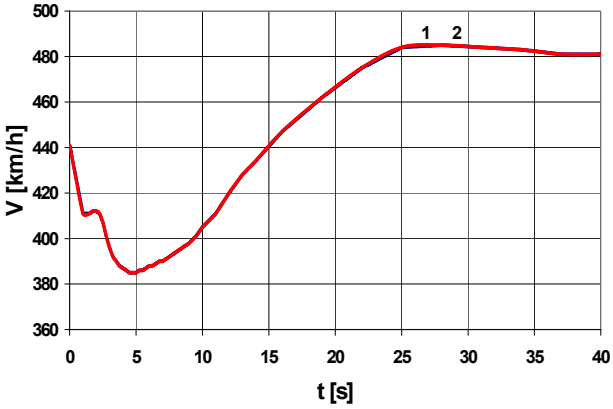


Fig.1 Flight velocity V(t)

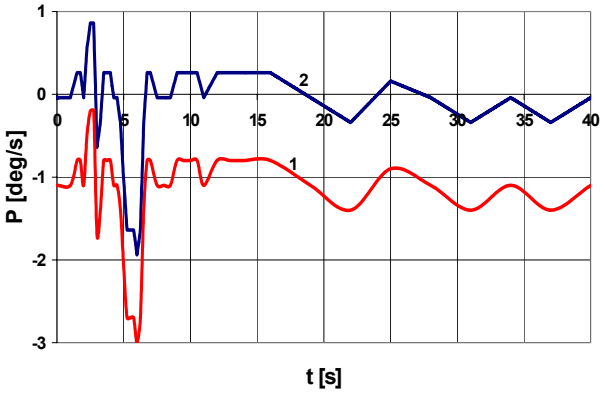


Fig.2 Rolling angular velocity P(t)

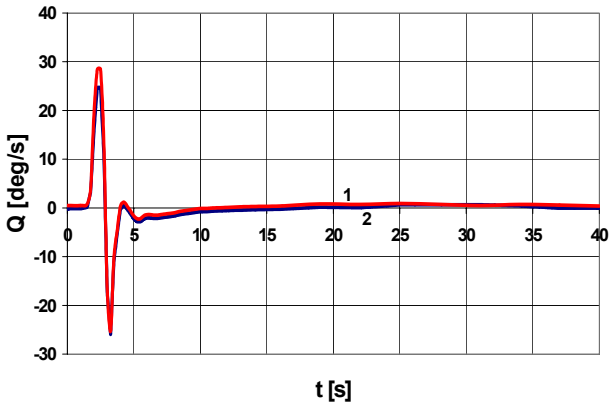


Fig.3 Pitching angular velocity Q(t)

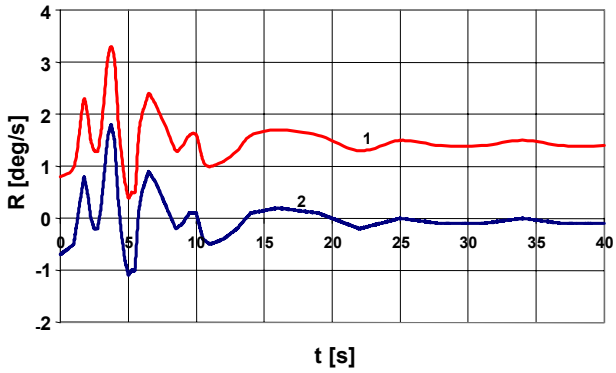


Fig.4 Yawing angular velocity R(t)

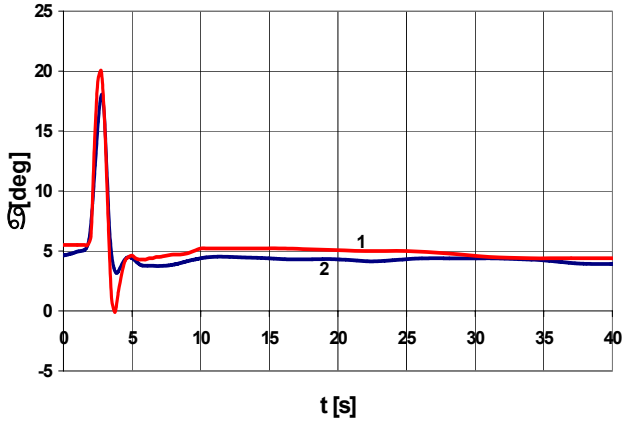


Fig.5 Angle of attack α(t)

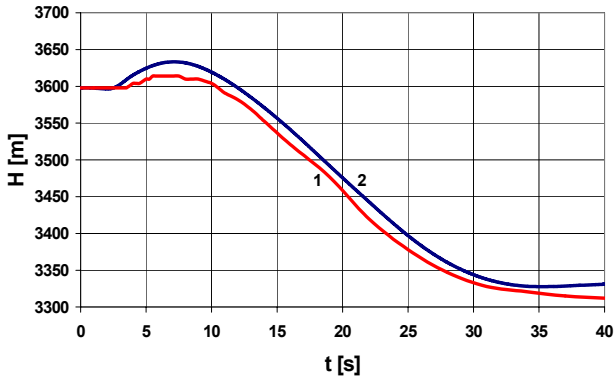


Fig.6 Flight altitude H(t)

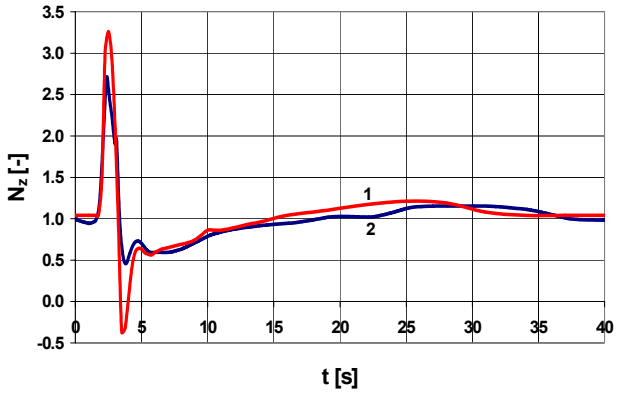


**Fig.7 Overload factor $N_z(t)$**

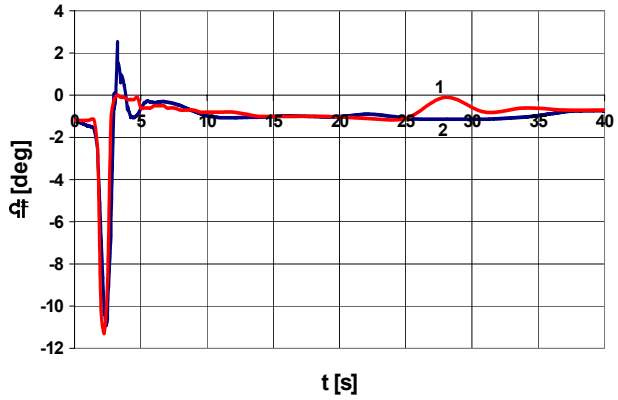


**Fig.8 Elevator deflection $\delta_H(t)$**

## 4.0 SIMULATION OF SELECTED AIRCRAFT SPATIAL MANOEUVRES

To illustrate efficiency of the applied inverse method of simulation, some results of numerical calculation for selected spatial manoeuvres are presented below. Time courses of various flight parameters were taken as constrains. But for all cases, the following rule was obligated: among four selected parameters, which were the constraints, two were the longitudinal parameters (two from $V$, $\alpha$, $Q$, $\Theta$ for an aeroplane or two from $U$, $W$, $Q$, $\Theta$ for a helicopter), and two other were connected with a lateral motion (two from $\beta$, $P$, $R$, $\Phi$, $\Psi$ for an aeroplane or two from $V$, $P$, $R$, $\Phi$, $\Psi$ for a helicopter). Selection of these parameters was performed in order to complete the description of a individual aircraft manoeuvre. Calculations were done for aeroplanes: the MiG-29 and TS-11 *Iskra*, respectively.

Significant works were also connected with simulations of the helicopter Nap-Of-The-Earth manoeuvres /NOE/. In compliance with the ADS-33 norm [7] a significant number of experimental investigations were performed for the Polish-designed *Sokol* helicopter. Flight tests followed numerical simulations of every manoeuvre. In this case the inverse technique was also applied to numerical prediction of a behaviour of the helicopter performing the NOE manoeuvres. A mathematical model with inertial cross-coupling was used. Motions of the blades were also considered.

These simulations enabled theoretical prediction of helicopter behaviour. Their results were analysed in details. Then, a scenario of a test flight was determined and the flight was performed. A lot of flight and

control parameters were recorded. After that, on the basis of these courses the way of the flight execution was discussed. Simultaneously, numerical reconstruction of the flight was done. This made possible to improve a pilotage technique. Objective estimations of the helicopter performances were obtained. They were compared with the ADS-33 norm.

Several manoeuvres were simulated. In this paper, one aeroplane manoeuvre and one helicopter manoeuvre are presented as examples.

### 4.1. Turn Manoeuvre

The turn is a typical manoeuvre of an aeroplane. Steady state flight was assumed as an initial condition. It was executed with velocity $V$=138.9 m/s (500 km/h). The angle of incidence was of $\alpha_0$=2.763$^0$ and the thrust was of $T_c$=3310 N. An assumption was taken that the velocity and the pitch angle of aeroplane were stable during the turn and equal to their initial values.

$$V(t)=138.9 \text{ m/s}=\text{const} \qquad (4.1)$$

$$\Theta(t)=\Theta_0=\alpha_0=2.763^0=\text{const} \qquad (4.2)$$

Two next constraints connected with lateral motion were as follows:

- the sideslip angle was equal to zero:

$$\beta(t)=0=\text{const} \qquad (4.3)$$

- changes of the roll angle $\Phi$ were determined by the following formula:

$$\Phi(t)=\begin{cases} 0 & \text{for } t<t_1 \text{ oraz } t>t_2+T_2 \\ \frac{\Phi_z}{16}\left(\cos 3\pi\frac{t-t_1}{T_1}-9\cos\pi\frac{t-t_1}{T_1}+8\right) & \text{for } t_1\le t<t_1+T_1 \\ \Phi_z & \text{for } t_1+T_1\le t\le t_2 \\ \Phi_z\left[1-\frac{1}{16}\left(\cos 3\pi\frac{t-t_2}{T_2}-9\cos\pi\frac{t-t_2}{T_2}+8\right)\right] & \text{for } t_2\le t\le t_2+T_2 \end{cases} \qquad (4.4)$$

where $\Phi_z$ is the maximum value of the roll angle, $t_1$ – time of the beginning of the manoeuvre, $T_1$ – period of the first phase of turn, $t_2$ – time of the beginning of the final phase of turn, $T_2$ – period of the final phase of turn.

The last constraint presents that the turn is realised by a roll of an airplane. During the time between $t_1$+$T_1$ and $t_2$ the airplane performs the turn with the steady roll angle. In the presented simulation, the following values were used: $\Phi_z=57^0$, $t_1=0s$, $T_1=5s$, $t_2=15s$, $T_2=5s$.

Results are presented in Figs 9÷15. They show that all constraints are fulfilled precisely. For instance Fig. 9 shows time course of the roll angle. It is in agreement with the formula (4.4).

Fig.9 and 10 tell that the right turn was performed. The direction change of 90$^0$ is visible. The turn is realized with the angle of attack greater than the steady state horizontal flight /Fig.11/. This is due to the fact that for the turn only the component of lift force balances the weight of airplane. Therefore it is necessary to increase the lift. The value of the angle of attack increases aerodynamic drag forces. To compensate the additional drag the thrust of engine has to be improved /Fig.12/.

Figures 13÷15 show other control signals, which are determined with inverse simulation (the thrust is the first one). Enter into and pull out from the turn is performed with ailerons /Fig.13/. To fly without any sideslipe angle the rudder has to be deflected all the time of the turn /Fig.14/. The elevator is also applied

/Fig.15/ because of the increased value of the incidence. For performing this manoeuvre it is necessary to keep handle of an aeroplane by using all the controls.

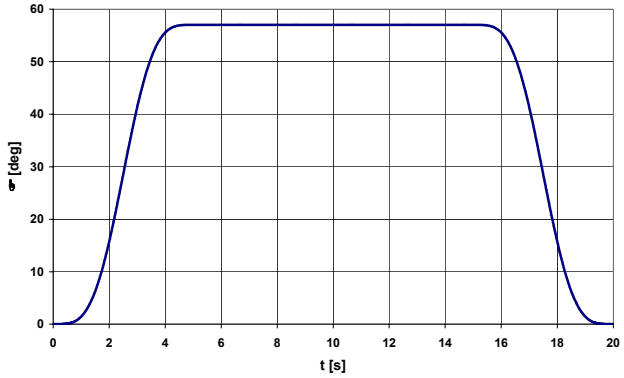


**Fig.9 Roll angle during turn manoeuvre Φ(t)**

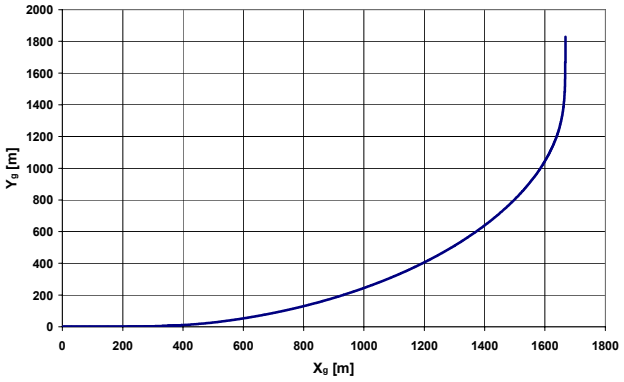


**Fig.10 Trajectory projection on $Ox_g$ $y_g$ plane**

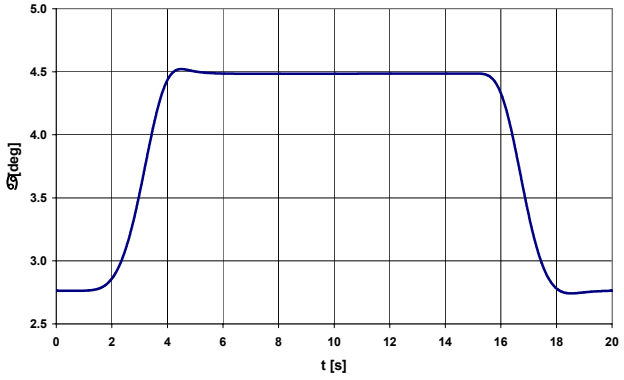


**Fig.11 Angle of attack during turn manoeuvre α(t)**

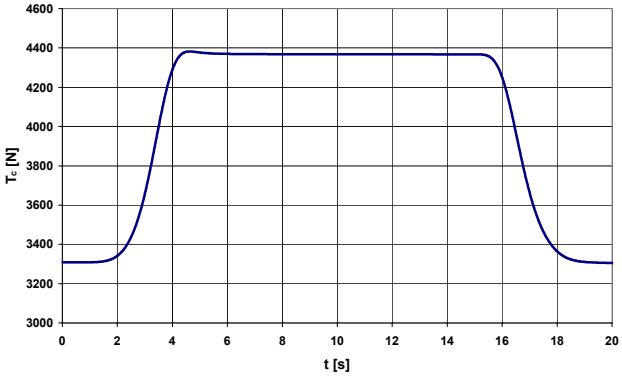


**Fig.12 Thrust during turn manoeuvre T(t)**

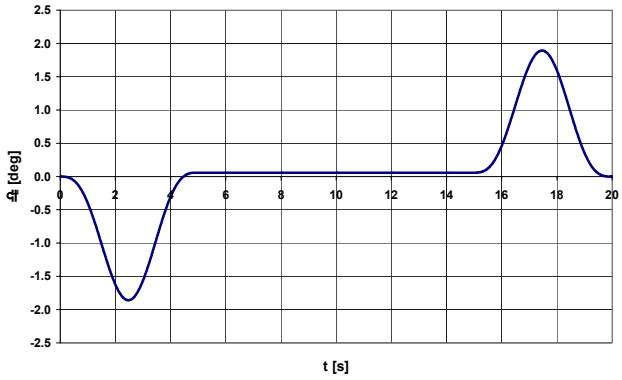


**Fig.13 Ailerons deflection $\delta_L(t)$**

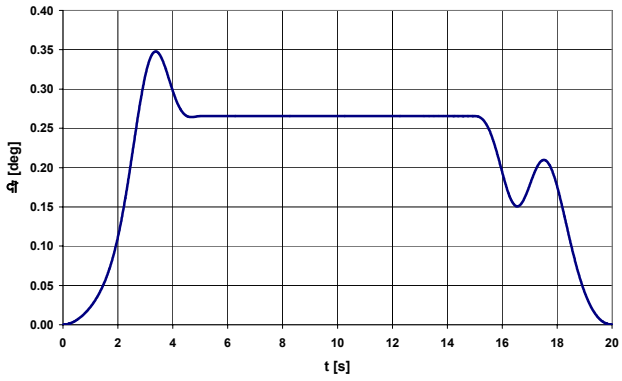


**Fig.14 Rudder deflection $\delta_V(t)$**

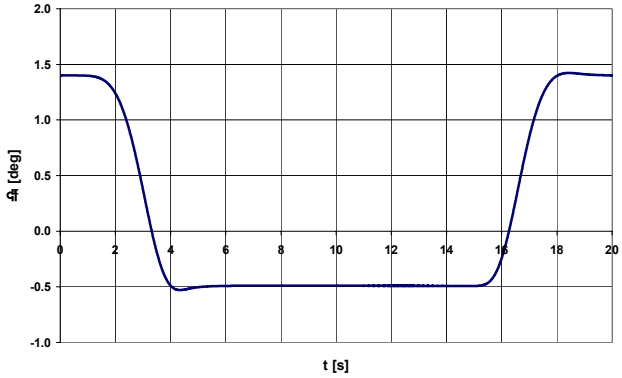


**Fig.15 Elevator deflection $\delta_H(t)$**

## 4.2 Hurdle-hop manoeuvre

The hurdle-hop is a terrain following manoeuvre. It is applied to avoid detection whilst passing obstacles at low level altitude in nap-of-the-earth flights. This manoeuvre should be performed symmetrically with sidestep constrained to be zero.

For the purpose of simulation it was assumed that the manoeuvre was performed on the vertical plane. It meant that yawing and rolling velocities were equal to zero.

$$P(t), Q(t) = 0 \qquad (4.5)$$

The two other constraints connected with the longitudinal motion were defined as follows:

- the pitching angular velocity:

$$Q = \begin{cases} 0 & for \quad t < t_{m1Q},\ t > t_{m4Q} + T_{d4Q} \\ \frac{Q_A}{16}\left(\cos 3\pi \frac{t - t_{m1Q}}{T_{d1Q}} - 9\cos\pi \frac{t - t_{m1Q}}{T_{d1Q}} + 8\right) & for \quad t_{m1Q} \le t < t_{m1Q} + T_{d1Q} \\ Q_A & for \quad t_{m1Q} + T_{d1Q} \le t < t_{m2Q} \\ Q_A - \frac{Q_A + Q_B}{16}\left(\cos 3\pi \frac{t - t_{m2Q}}{T_{d2Q}} - 9\cos\pi \frac{t - t_{m2Q}}{T_{d2Q}} + 8\right) & for \quad t_{m2Q} \le t < t_{m2Q} + T_{d2Q} \\ -Q_B & for \quad t_{m2Q} + T_{d2Q} \le t < t_{m3Q} \\ -Q_B + \frac{Q_B + Q_C}{16}\left(\cos 3\pi \frac{t - t_{m3Q}}{T_{d3Q}} - 9\cos\pi \frac{t - t_{m3Q}}{T_{d3Q}} + 8\right) & for \quad t_{m3Q} \le t \le t_{m3Q} + T_{d3Q} \\ Q_C & for \quad t_{m3Q} + T_{d3Q} \le t < t_{m4Q} \\ Q_C - \frac{Q_C}{16}\left(\cos 3\pi \frac{t - t_{m4Q}}{T_{d4Q}} - 9\cos\pi \frac{t - t_{m4Q}}{T_{d4Q}} + 8\right) & for \quad t_{m4Q} \le t \le t_{m4Q} + T_{d4Q} \end{cases} \qquad (4.6)$$

- the altitude of flight:

$$H = \begin{cases} 0 & for \quad t < t_{m1H} \\ \frac{H_1}{16}\left(\cos 3\pi \frac{t - t_{m1H}}{T_{d1H}} - 9\cos\pi \frac{t - t_{m1H}}{T_{d1H}} + 8\right) & for \quad t_{m1H} \le t < t_{m1H} + T_{d1H} \\ H_1 & for \quad t_{m1H} + T_{d1H} \le t < t_{m2H} \\ H_1 + \frac{H_1 - H_2}{16}\left(\cos 3\pi \frac{t - t_{m2H}}{T_{d2H}} - 9\cos\pi \frac{t - t_{m2H}}{T_{d2H}} + 8\right) & for \quad t_{m2H} \le t < t_{m2H} + T_{d2H} \\ H_2 & for \quad t \ge t_{m2H} + T_{d2H} \end{cases} \qquad (4.7)$$

These formulas were derived on the basis of the time courses recorded during the beginning of the test flight /Figs.16, 17/. The following values were taken into consideration:

$t_{m1H} = 2s$ , $T_{d1H} = 3.5s$ , $t_{m2H} = 5.5s$ , $T_{d2H} = 4.5s$ , $H_1 = 17m$ , $H_2 = 5m$ , $t_{m1Q} = 1.5s$ , $T_{d1Q} = 1.25s$ ,
$t_{m2Q} = 2.75s$ , $T_{d2Q} = 1.5s$ , $t_{m3Q} = 5.2s$ $T_{d3Q} = 3.25s$ , $t_{m4Q} = 8.7s$ , $T_{d4Q} = 1.75s$ ,
$Q_A = 0.3142rad/s$ , $Q_B = 0.2746rad/s$ , $Q_C = 0.1745rad/s$ .

Figures 18 and 19 show that the constraints of motion are realised exactly. Also other computed flight parameters, which are not constraints are in satisfactory agreement with other recorded parameters: – flight velocity *V(t)* /Fig.18/ , – collective pitch angle $\Theta_0(t)$ /Figs.21, 22/, flapping motion of blades $\beta(t)$ /Figs.23, 24/.

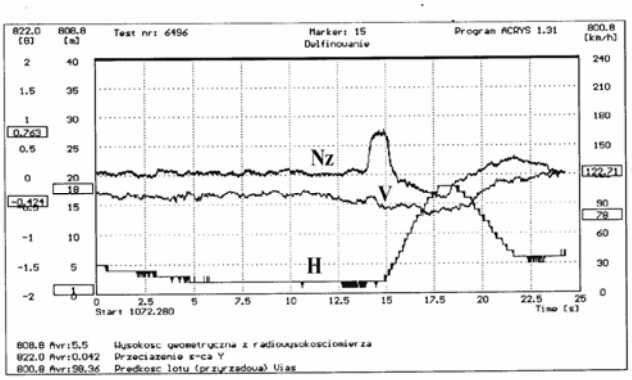


**Fig.16 Recorded flight velocity, altitude and overload**

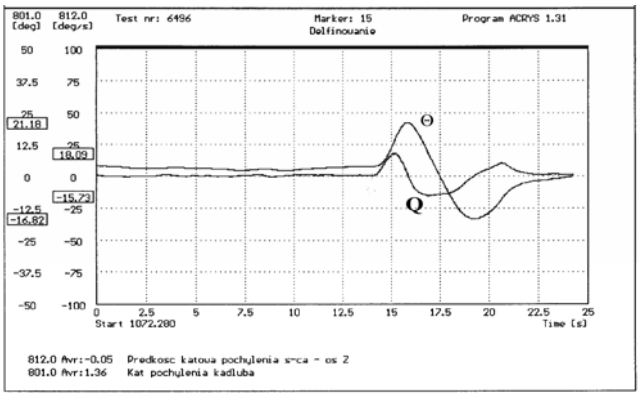


**Fig.17 Recorded pitching velocity and pitch angle**

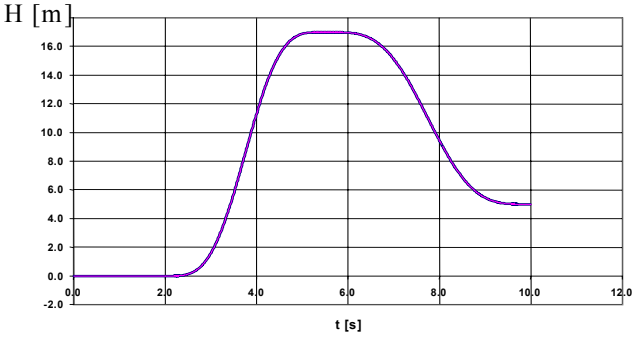


**Fig.18 Flight altitude H(t) (simulation)**

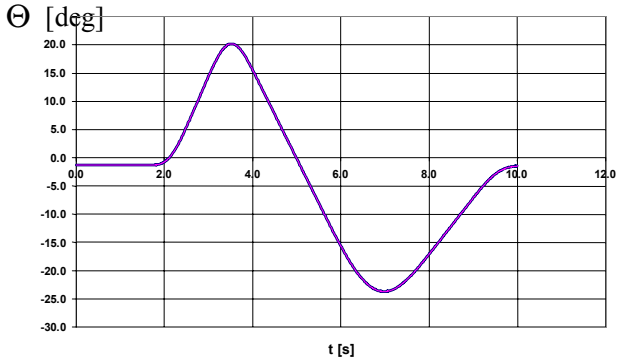


**Fig.19 Pitch angle Θ(t) (simulation)**

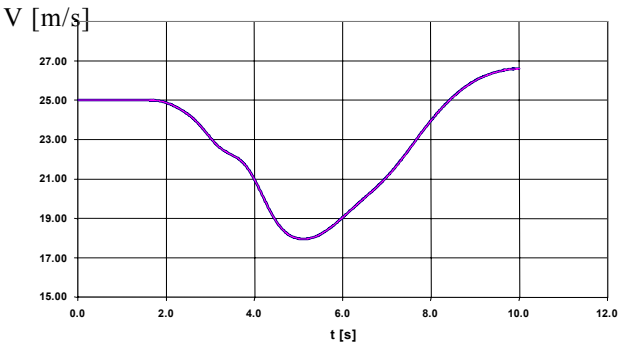


**Fig.20 Flight velocity V(t) (simulation)**

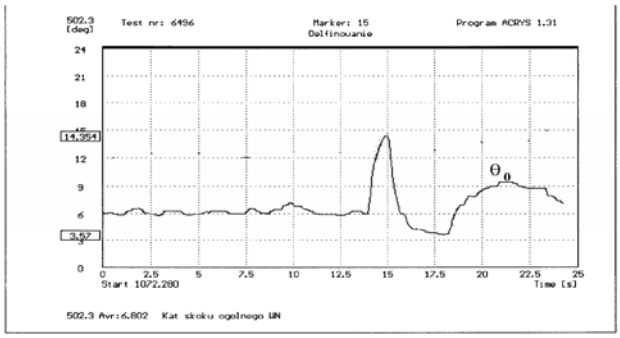


**Fig.21 Collective pitch Θ$_0$(t) (recorded)**

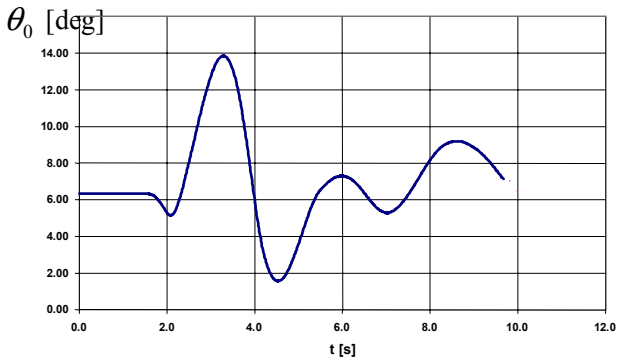


**Fig.22 Collective pitch Θ$_0$(t) (simulation)**

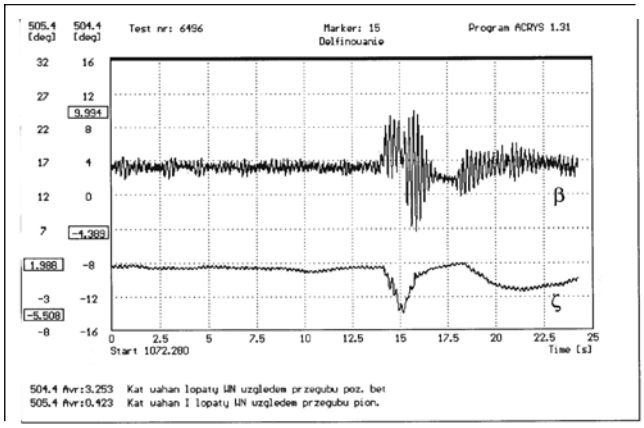


**Fig.23 Flapping motion β(t) (recorded)**

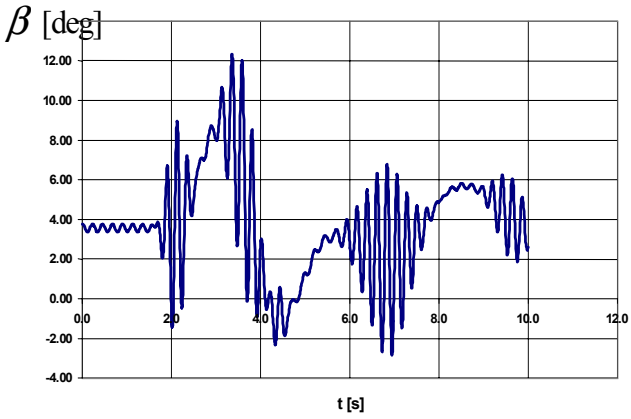


**Fig.24 Flapping motion β(t) (simulation)**

## 5.0 RECONSTRUCTION OF AN AIRCRAFT ACCIDENT

Numerical reconstruction of an aircraft crash was one of the fundamental works. On 11 November 1998 the Polish-designed trainer TS-11 *Spark* crashed during the routine flight operation. Two pilots lost their life. Unfortunately the TS-11 was not equipped with the Flight Data Recorder (FDR). Therefore the time history of a flight velocity obtained from a ground radar station was the only one objective data describing this flight path. Reports of eyewitnesses were the other source of information about the critical phase of flight. On the basis of the available information two hypotheses were formulated:

- the aircraft was in operational working order and the pilot made a mistake,
- an icing phenomenon was the main reason of the crash.

These hypotheses were verified making use of a standard 6 degrees-of-freedom model of plane flight dynamics. Previously that model had been verified by comparing results of simulations with data from the FDR. It was shown in paragraph 3 of this work.

**Assumptions taken for simulations**

On the basis of information from various sources the following assumptions on the critical phase of the flight were taken:

1. The initial conditions /beginning of the final 35 sec. long period/:
   - the steady state horizontal flight at altitude of 100 meters;
   - the flight velocity 145m/s (522km/h).
2. The course of events:
   - a climb at about 500m;
   - a deep right turn with increasing pitch, bank and roll angles and flight velocity.
3. The final configuration of the aircraft:
   - the pitch angle $\Theta = 50^0$
   - the bank angle $\Phi = 125^0$
   - the roll angle $\Psi = 143^0$
   - the final velocity 172÷180m/s (620-650 km/h )
4. The distance from the initial trajectory to the crash point: 750÷952m.

These assumptions were formulated on the basis of eyewitnesses reports and on the radiolocation data /Fig.25/. Therefore the time history of a flight velocity was only one objective data about the flight.

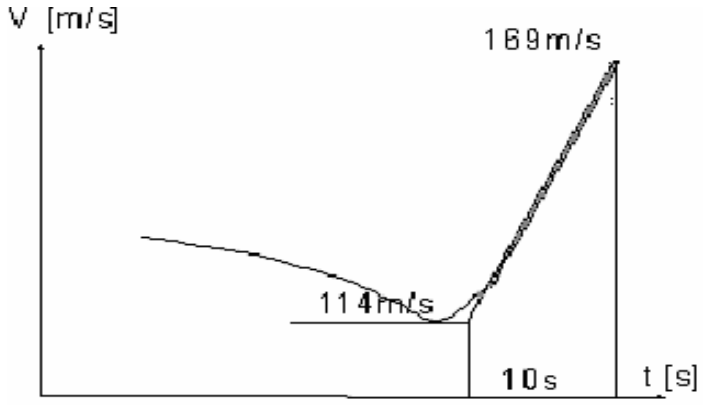


**Fig.25 The flight velocity /radiolocation data/**

**Icing influence on aerodynamic characteristics**

To test the latter hypothesis i.e. aircraft icing as a main reason of the crash, the basic aerodynamic characteristics were modified. It was done by utilisation of data available from literature /[8] ÷[10]/ and of our own [11] investigations. These investigations were performed in the Institute of Aviation Technology of the Military University of Technology. The obtained results are comparable to those taken from other sources. Exemplary data from wind tunnel are shown in Figs.26 and 27.

Detailed analysis shows that the icing phenomenon results in:

1. Extensive degradation of the lift coefficient $C_L$;
2. Decrease of the derivative $\frac{dC_L}{d\alpha}$;
3. Decrease of the critical angle of attack;

4. Increase of the derivative $\frac{dC_m}{d\alpha}$;
5. Increase of the pitch coefficient $C_m$;
6. Increase of the drag coefficient $C_D$.

Descriptions of these investigations can be found in [11]. On this base all initially taken aerodynamic coefficients were modified.

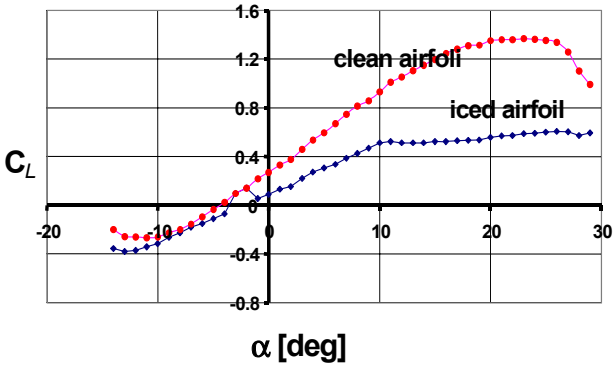


**Fig.26 Lift coefficient $C_L$**

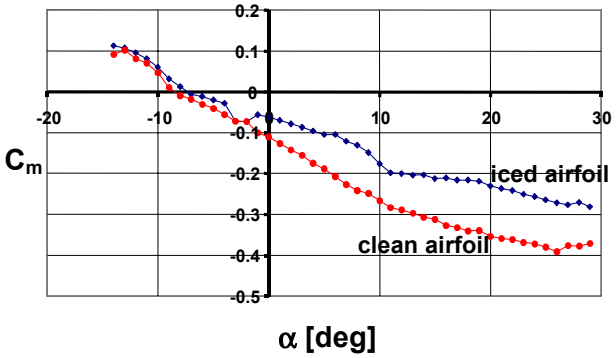


**Fig.27 Lift coefficient $C_m$**

**Simulation of iced aeroplane flight**

It was assumed that the icing phenomena appeared at the twenty fifth second during the climb. The aircraft was at 250 meters above the initial altitude of the flight. All aerodynamic characteristics changed as it is described above.

Control inputs were obtained using the inverse technique on the basis of assumed time histories of: - the velocity, the altitude,

- the pitch angle and the bank angle.

Results of simulations are presented in Figs.28÷39.

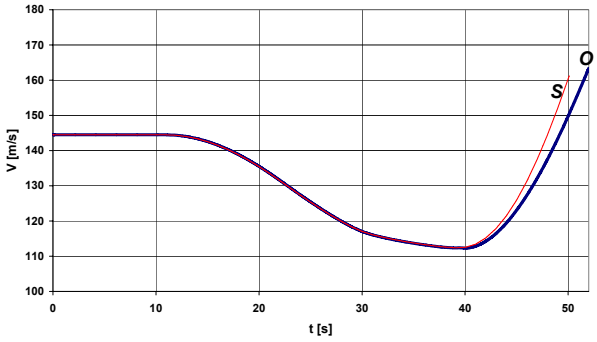


Fig.28 Flight velocity V (s – clear; o – iced)

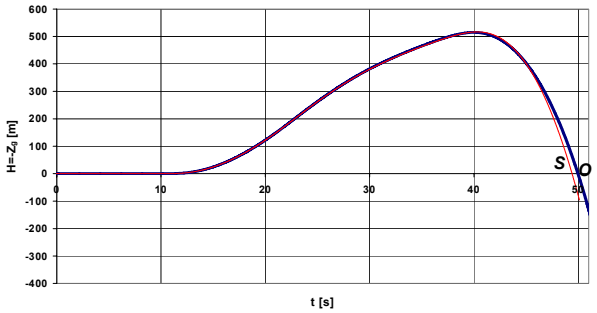


Fig.29 Flight altitude $H=-z_g$ (s – clear; o – iced)

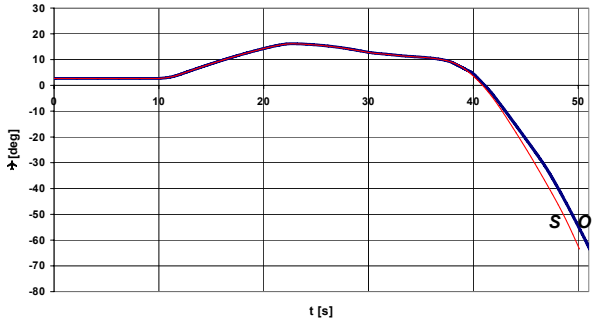


Fig.30 Pitch angle $\Theta$ (s – clear; o – iced)

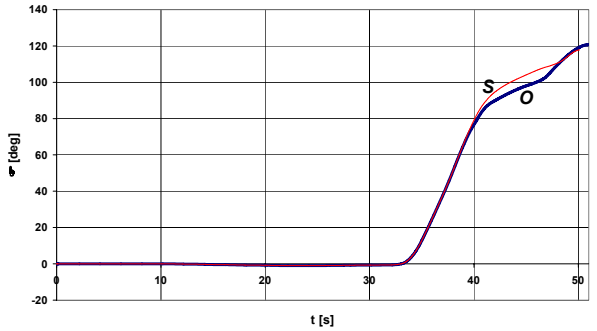


Fig.31 Roll angle $\Phi$ (s – clear; o – iced)

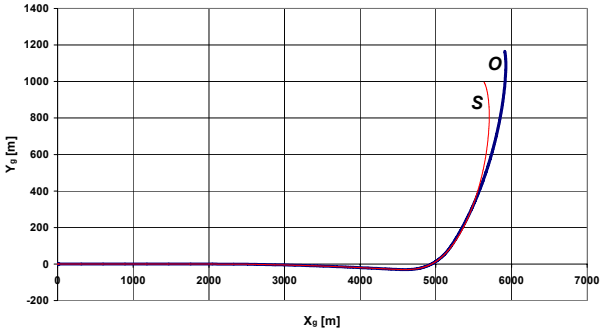


Fig.32 Trajectory of flight (s – clear; o – iced)

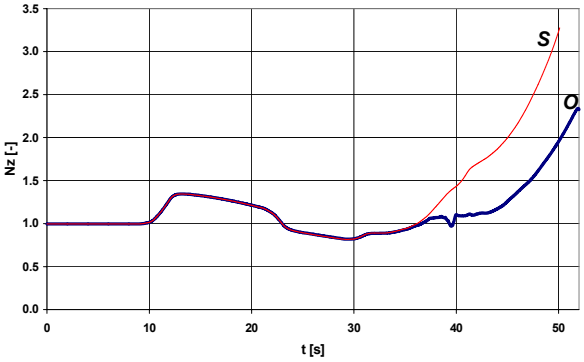


Fig.33 Overload factor (s – clear; o – iced)

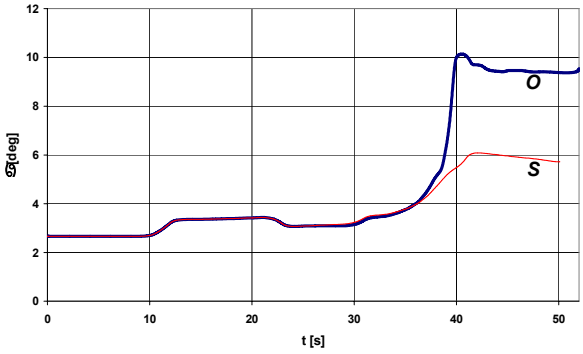


Fig.34 Angle of attack $\alpha$ (s – clear; o – iced)

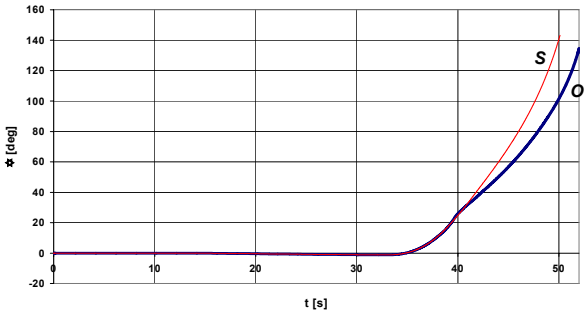


Fig.35 Yaw angle $\Psi$ (s – clear; o – iced)

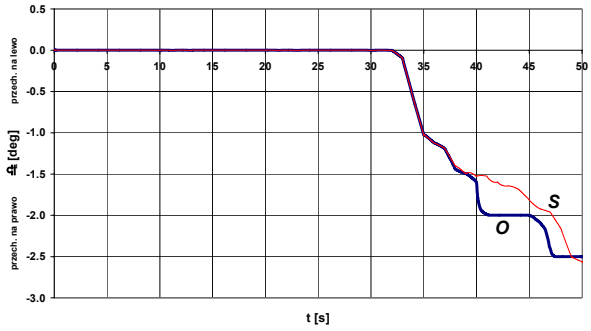


Fig.36 Ailerons deflection $\delta_L(t)$ (s – clear; o – iced)

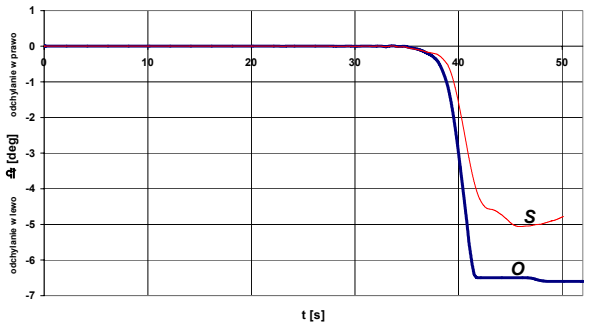


Fig.37 Rudder deflection $\delta_V(t)$ (s – clear; o – iced)

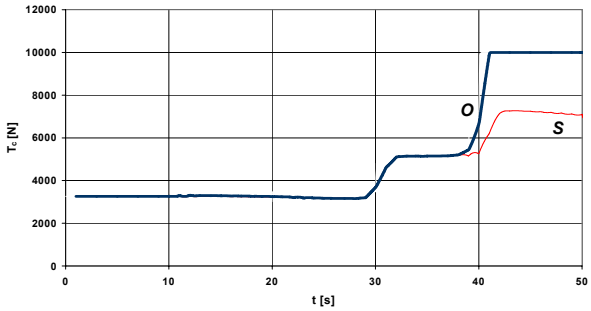


Fig.38 Thrust T (s – clear; o – iced)

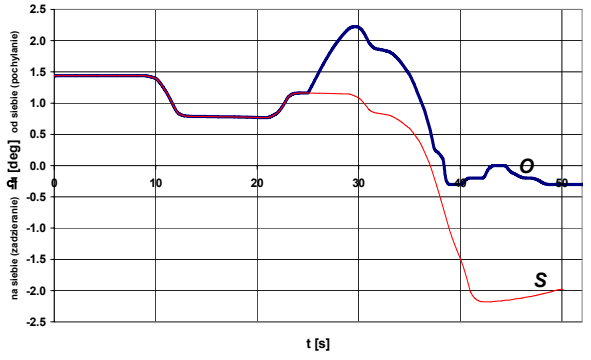


Fig.39 Elevator deflection $\delta_H(t)$ (s – clear; o – iced)

The final configuration of the airplane was determined with the accuracy shown in Table 1.

**Table 1 Crucial parameters of the final configuration**

| No | Flight parameter | Assumed value | Calculated value | Discrepancy |
|---|---|---|---|---|
| 1 | Flight velocity | 172÷180m/s | 163m/s | 9m/s |
| 2 | Pitch nagle | $50^0$ | $61^0$ | $11^0$ |
| 3 | Bank angle | $125^0$ | $120^0$ | $5^0$ |
| 4 | Yaw angle | $143^0$ | $138^0$ | $5^0$ |
| 5 | Crash point distance | 750÷952m | 1170m | 420÷218m |
| 6 | Maximum altitude | 500m | 620m | 120m |

The presented comparison /Tab.1/ shows that the calculated final values of flight parameters are close to the assumed ones. It concerns particularly all angles describing the spatial orientation of the aircraft. Courses of: the flight velocity, the pitch angle and the roll angle are similar as in the case of the clean aircraft. But the angle of attack /Fig.34/ is about $3^0$ greater during the final phase of flight. The sideslip angle (not shown) is greater too. It means that the iced aircraft, in respect to the velocity vector, is situated differently from the clean aircraft. Fig.33 shows that in the case of the icing the flight is performed with the smaller overload – the dynamics of the manoeuvre is perceived weakier.

The fundamental contrast is visible for the thrust /Fig.38/ and the elevator angle /Fig.39/. For the iced aircraft the thrust is equal to its maximum value. It is caused by the increase of the drag force. The drag increases because the angle of attack is greater and the aircraft surface is rough. The detailed analysis of the elevator displacement shows that at the initial phase of icing it was in order to push the stick to compensate the pitching up moment. Next the stick was pulled but its displacement was smaller than in the case of efficient aircraft.

The analysis of figures 36 and 37 proves that the assumed trajectory of flight could be obtained only, when the aircraft was controlled with ailerons and the rudder. The control inputs were similar to these derived for the efficient aircraft.

## 6.0 CONCLUSIONS

On the basis of the obtained results the following conclusions can be formulated:

1. If the airplane was aerodynamically efficient, obtaining of the final point of the trajectory would be possible only with conscious control of all control parameters. It means that the pilot made an error.
2. If the icing occurred, the aircraft would react very quickly decreasing the lift force, pitching the nose up and yawing left. The crew reacted properly.

The analysis proved, that the inverse technique is the efficient one for the reconstruction of a flight trajectory even when the data is insufficient.

## 7.0 REFERENCES

[1] Kowaleczko G., *Inverse problem aircraft in flight dynamics*, Military University of Technology, 2003, ISBN 83-98399-30-X, (*in Polish*);

[2] Kowaleczko G., *An Improved Numerical Approach for Inverse Simulations of Aircraft Manoeuvres*, Journal of Theoretical and Applied Mechanics, No.1, vol. 39, 2001;

[3] Kowaleczko G., Sobieraj W., *Reconstruction of an Aircraft Accident Using an Inverse Technique*, AIAA Paper-2003-0581;

[4] Goszczyński J., Kowaleczko G., Maryniak J., *Reconstruction of Flight Control Making Use of Inverse Simulation,* Mechanika w Lotnictwie (ML-IX 2000), wyd. PTMTS, 2000, (*in Polish*);

[5] G. Kowaleczko, *Simulated and Experimental Investigation of the Nap-of-The Earth Manoeuvres for a Helicopter*, Proceedings of 26th European Rotorcraft Forum, Haga-Holland, 26-29.09.2000;

[6] Berezanski J., Kowaleczko G., *Numerical Prediction of Behaviour of a Helicopter performing the Nap-of-the-Earth Manoeuvres and its Experimental Verification*, Proceedings of 27th European Rotorcraft Forum, Moscow, Russia, 11-14.09.2001;

[7] *Aeronautical Design Standard – Handling Qualities Requirements for Military Rotorcraft*, United States Army Aviation and Troop Command, St. Louis, July 1994

[8] Cebeci T., Effect of Ice on Airfoil at High Reynolds at High Reynolds Number, AIAA Journal, Vol.33, No. 7, 1995.

[9] Lee S., Kimm H., Bragg M., *Investigation of Factors That Influence Iced – Airfoil Aerodynamics*, AIAA 2000-0099, Proceedings of 38th Aerospace Sciences Meeting & Exhibit, Reno, USA, 10÷13 January 2000.

[10] Bragg M., Hutchinson T., Merret J., Pokhariyal D., *Effect of Ice Accretion on Aircraft Flight Dynamics*, AIAA 2000-0360, Proceedings of 38th Aerospace Sciences Meeting & Exhibit, Reno, USA, 10÷13 January 2000

[11] Frant M., Kowaleczko G., Sobieraj W., *The Effect of Icing on the Flight Characteristics of an Aircraft*, Transaction of the Institute of Aviation, No. 167, Warsaw, 2001, (*in Polish*).